Journal of Alzheimer's Disease 85 (2022) 1667–1676
DOI 10.3233/JAD-215072
IOS Press

Impact of 40 Hz Transcranial Alternating Current Stimulation on Cerebral Tau Burden in Patients with Alzheimer's Disease: A Case Series

Maeva Dhaynaut[a,1], Giulia Sprugnoli[b,1], Davide Cappon[b], Joanna Macone[b], Justin S. Sanchez[a,c], Marc D. Normandin[a], Nicolas J. Guehl[a], Giacomo Koch[d], Rachel Paciorek[b], Ann Connor[b], Daniel Press[b], Keith Johnson[a,c], Alvaro Pascual-Leone[e,f], Georges El Fakhri[a,1,*] and Emiliano Santarnecchi[a,b,1,*]

[a]*Gordon Center for Medical Imaging, Department of Radiology, Massachusetts General Hospital, Harvard Medical School, Boston, MA, USA*
[b]*Berenson-Allen Center for Noninvasive Brain Stimulation, Department of Neurology, Beth Israel Deaconess Medical Center, Harvard Medical School, Boston, MA, USA*
[c]*Division of Nuclear Medicine and Molecular Imaging, Department of Radiology, Massachusetts General Hospital, Harvard Medical School, Boston, MA, USA*
[d]*Santa Lucia Foundation, Rome, Italy*
[e]*Hinda and Arthur Marcus Institute for Aging Research and Deanna and Sidney Wolk Center for Memory Health, Hebrew SeniorLife, Boston, MA, USA*
[f]*Department of Neurology, Harvard Medical School, Boston, MA, USA*

Accepted 26 November 2021
Pre-press 21 December 2021

Abstract.
Background: Alzheimer's disease (AD) is characterized by diffuse amyloid-β (Aβ) and phosphorylated Tau (p-Tau) aggregates as well as neuroinflammation. Exogenously-induced 40 Hz gamma oscillations have been showing to reduce Aβ and p-Tau deposition presumably *via* microglia activation in AD mouse models.
Objective: We aimed to translate preclinical data on gamma-induction in AD patients by means of transcranial alternating current stimulation (tACS).
Methods: Four participants with mild-to-moderate AD received 1 h of daily 40 Hz (gamma) tACS for 4 weeks (Monday to Friday) targeting the bitemporal lobes (20 h treatment duration). Participant underwent Aβ, p-Tau, and microglia PET imaging with [^{11}C]-PiB, [^{18}F]-FTP, and [^{11}C]-PBR28 respectively, before and after the intervention along with electrophysiological assessment.
Results: No adverse events were reported, and an increase in gamma spectral power on EEG was observed after the treatment. [^{18}F]-FTP PET revealed a significant decrease over 2% of p-Tau burden in 3/4 patients following the tACS treatment, primarily involving the temporal lobe regions targeted by tACS and especially mesial regions (e.g., entorhinal cortex). The amount of intracerebral Aβ as measured by [^{11}C]-PiB was not significantly influenced by tACS, whereas 1/4 reported a significant decrease of microglia activation as measured by [^{11}C]-PBR28.

[1]These authors contributed equally to this work.

*Correspondence to: Emiliano Santarnecchi, PhD, Gordon Center for Medical Imaging, Department of Radiology, Massachusetts General Hospital, Harvard Medical School, Boston, MA, USA. Tel.: +1 617 667 0326; E-mail: esantarnecchi@mgh.harvard.edu and Georges El Fakhri, PhD, DABR, Director, Gordon Center for Medical Imaging, Co-Director, Division of Nuclear Medicine & Molecular Imaging, Massachusetts General Hospital, Nathaniel & Diana Alpert Professor of Radiology, Harvard Medical School, Boston, MA, USA. Tel.: +1 617 953 5085; E-mail: mwstpierre@mgh.harvard.edu.

ISSN 1387-2877/$35.00

Conclusion: tACS seems to represent a safe and feasible option for gamma induction in AD patients, with preliminary evidence of a possible effect on protein clearance partially mimicking what is observed in animal models. Longer interventions and placebo control conditions are needed to fully evaluate the potential for tACS to slow disease progression.

Keywords: Amyloid, dementia, electroencephalography, gamma, neurostimulation, positron-emission tomography, protein clearance, protein misfolding, tau, transcranial electrical stimulation

INTRODUCTION

Alzheimer's disease (AD) is the leading cause of dementia, accounting for 60–80% of all dementia cases, with its incidence and prevalence projected to increase [1]. Therapeutic options are very limited, with a few pharmacologic interventions that can temporarily slow down the memory loss and cognition impairment (e.g., cholinesterase inhibitors), but no available disease modifying treatments [2]. AD is characterized by diffuse extracellular amyloid-β (Aβ) plaques and phosphorylated Tau (p-Tau) intraneuronal aggregates. These aggregates interfere with neuron-to-neuron communication at the synaptic level, leading to neurodegeneration. Protein aggregates also cause the activation of microglia, the brain resident macrophage cells responsible of the neuroinflammation that, in turn, further promotes the neurodegeneration [3, 4]. Recent PET imaging studies suggest that progressive Aβ deposition can begin up to 20 years before the onset of clinical symptoms and stabilizes around the time that clinical symptoms become prominent [5]. p-Tau accumulates particularly in the mesial temporal lobes even in the absence of Aβ and spreads outside the temporal lobes following a different spatial trajectory than Aβ [6, 7]. Importantly, neurodegeneration and clinical symptoms are strongly correlated with the spread of p-Tau [6]. Consequently, evidence suggests that both Aβ and p-Tau play a critical role in AD pathogenesis even if their interdependency has not been fully disentangled yet [3, 8], making interventions that reliably and safely decrease intracerebral Aβ and p-Tau burden of marked clinical importance (Fig. 1).

Another consistent finding in patients with AD is a relative attenuation of fast oscillatory brain activity in the 30–80-Hz range, known as "gamma" activity [9]. Crucially, some of the regions whose oscillatory activity in the gamma band, as well as fMRI connectivity, are altered in AD patients (i.e., regions of the default mode network, see Fig. 1), are the same regions affected by Aβ (i.e., lateral temporal lobe, angular gyrus, precuneus and medial frontal cortex), and partially by p-Tau (i.e., temporal pole, lateral temporal lobe, and angular gyrus), suggesting a link between oscillatory neural activity and protein accumulation [8, 10]. Recent preclinical work has demonstrated that exogenously-induced 40 Hz gamma oscillations can reduce Aβ deposition *via* microglia activation and may also reduce p-Tau levels in a mouse model of AD (5XFAD) [11]. In presymptomatic AD mice, induction of gamma activity prevents subsequent neurodegeneration and behavioral impairments [12]. Those results suggest that gamma induction may represent a novel therapeutic approach for AD [13]. Therefore, in the present case series study we aimed to test the safety and feasibility of translating the aforementioned preclinical findings on gamma induction to patients with AD, utilizing transcranial alternating current stimulation (tACS) as a tool to noninvasively entrain gamma oscillations, and PET imaging to assess protein clearance and neuroinflammation. tACS is a noninvasive brain stimulation technique able to entrain the underlying neuronal population by means of low-amplitude electrical current delivered at a specific frequency (e.g., 40 Hz) over the scalp [14]. Neural entrainment is thought to promote oscillatory activity at the stimulation frequency and ultimately potentiate the cognitive or sensory functions supported by the targeted region and specific oscillatory activity [15, 16]. Interest on potential tACS effects on glial cells of the brain (i.e., microglia) have begun to arise recently, giving new hope for the treatment of neurodegenerative disorders [13].

In the present pilot trial, 40 Hz tACS was administered 1 h daily for 4 weeks (Monday to Friday) in a sample of mild-to-moderate AD patients, focusing the stimulation on the temporal lobes bilaterally. Longitudinal PET imaging was performed before and after the tACS treatment via C-Pittsburgh Compound B ([^{11}C]-PiB) to evaluate Aβ load, [^{18}F]-Flortaucipir ([^{18}F]-FTP) to quantify p-Tau pathology, and [^{11}C]-PBR28 to assess microglia activation. The annual rate of change in global and regional Aβ and p-Tau ratio is rarely decreasing and is generally either

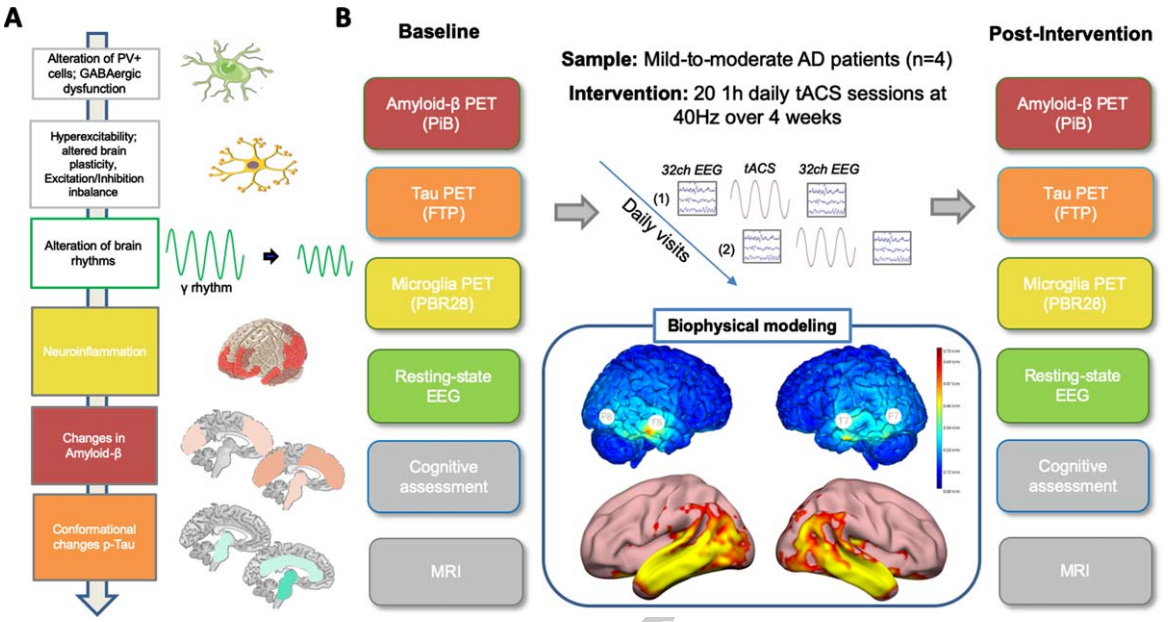

Fig. 1. Study Design. A) A simplified conceptual framework of the neuropathophysiology of AD is shown, describing the potential cascade involving interneuron dysfunction, altered excitation/inhibition balance, alterations of brain rhythms, neuroinflammatory response and protein accumulation. B) An attempt to map the different levels of the model directly in AD patients was made in the study design, with repeated EEG, amyloid-β, p-Tau and microglia PET imaging before and after the tACS treatment course. Neuroimaging and cognitive data were collected as well. Biophysical modeling displays the focus on bilateral temporal lobes and the resulting induced electrical field closely resembling p-Tau and amyloid-β accumulation.

nonsignificant or positive, typically on the order of 0.05 units/year, and asymptotes in patients with cognitive deficits and high Aβ and p-Tau levels [5, 17, 18]. Major spontaneous changes seem unlikely over the short time period between baseline and post-tACS treatment, allowing to capture potential beneficial effects of gamma-inducing tACS.

MATERIALS AND METHODS

Protocol

Five Aβ-positive patients with mild-to-moderate dementia due to AD were enrolled (Mini-Mental Score Examination (MMSE) = 22.20, SD = 4.5; male = 3; mean age = 70.2) and underwent 4 weeks (Monday to Friday, 20 sessions of 1 h daily) of tACS at 40 Hz targeting the bilateral temporal lobes in hospital settings (Fig. 1). One participant did not complete the post stimulation evaluation due to scheduling issues, therefore was excluded from the analysis (final sample $N = 4$; mean age = 76 years, male = 3; MMSE = 20.7, SD = 3.6). For more information on the sample including education, *APOE*, and BDNF status, see Table 1.

tACS uses low amplitude (usually delivered with a maximum of 2 mA per electrode) alternating sinusoidal currents *via* scalp electrodes to modulate cortical rhythmic activity in a frequency-specific manner [19, 20]. Bitemporal tACS was conceived as a way to induce focal stimulation over the temporal lobes given the typical Aβ and p-Tau protein distribution in these regions in the AD brain [6, 21], and on the basis of prior work by the PI using 40 Hz tACS in humans [15, 16, 22, 23]. Participant underwent baseline (pre-tACS) and follow-up (post-tACS) assessments composed of Aβ, p-Tau, and microglia PET imaging measured via [^{11}C]-PiB, [^{18}F]-FTP, and [^{11}C]-PBR28 on a Discovery MI (GE Healthcare) PET/CT scanner remaining below the limit of 50 mSv/year (36.9 mSv total study dose) as per the current safety guidelines on research exposure, along with cognitive testing and electroencephalography. [^{11}C]-PiB is an agent that binds specifically to Aβ [24], whereas [^{18}F]-FTP (previously known as T807 or AV-1451) binds with high affinity and selectivity to aggregated p-Tau pathology [25]. [^{11}C]-PBR28, a potent antagonist for mitochondrial translocator protein (TSPO), known to be upregulated in reactive microglia, demonstrates a good correlation between activated microglia and AD pathology [26].

Table 1
ADAS-Cog, Alzheimer's Disease Assessment Scale-Cognitive Subscale; BDNF, brain-derived neurotrophic factor; F, female; M, male; MMSE, Mini-Mental State Examination

Study ID	Age	Sex	Dominant Hand	Years of Education	Race	Ethnicity	MMSE baseline	ADAS-Cog baseline	*APOE* status	BDNF polymorphism
Sbj 001	84	M	Right	Master's Degree	White	Non-Hispanic	18	29	ε3/ε3	Val/Val
Sbj 002	73	F	Right	Master's Degree	White	Non-Hispanic	19	30	ε4/ε4	Val/Met
Sbj 003	84	M	Left	PhD	White	Non-Hispanic	20	14	ε3/ε4	Val/Val
Sbj 004	64	M	Right	Master's Degree	White	Non-Hispanic	26	18	ε4/ε4	Val/Val

At baseline and after the tACS treatment, patients underwent a cognitive assessment including measures of global cognition with specific focus on memory (Alzheimer's Disease Assessment Scale-Cognitive Subscale (ADAS-Cog) [27], baseline mean = 22.75, SD = 8.2; MMSE [28], baseline mean = 20.7, SD = 3.6; Montreal Cognitive Assessment (MoCA) [29], baseline mean = 13.25, SD = 4.1), and measures of functional ability and independence (Activities of Daily Living (ADL) [30], baseline mean = 70, SD = 2.6), to monitor safety of the proposed high-density tACS treatment regime also considering recent treatment-associated cognitive worsening reported for interventions targeting Aβ clearance pathways [31]. Additional details related to inclusion/exclusion criteria and cognitive assessment tools are reported as part of the Supplementary Material.

All participants gave written informed consent prior to participating in the study, registered on ClinicalTrials.gov (NCT03412604; PI Santarnecchi E). Patient's capacity to consent was established by a neurologist on the basis of the MMSE score and clinical evaluation during the consenting study visit. The research proposal and associated methodologies were approved by the local ethics committees (Beth Israel Deaconess Medical Center and Massachusetts Medical Center) in accordance with the principles of the Declaration of Helsinki.

tACS stimulation and EEG analysis

Stimulation was delivered at 40 Hz for 1 h using a Starstim 32-channels brain stimulation device (Neuroelectrics, Barcelona, Spain) in the morning for all participants, with each session starting between 8 to 12AM according to individual patients' schedules (Monday to Friday, 4 weeks, 20 tACS sessions in total). At the beginning of each session, the Starstim system was set up to stimulate both temporal lobes approximately corresponding to T8-T7 and P8-P7 in the 10/20 EEG system with a maximum intensity of 2 mA for each electrode and 4 mA total across all electrodes (Fig. 1), and impedance was checked. The daily tACS sessions started with resting-EEG recording (5' eyes open, 5' eyes closed), followed by 1 h of tACS at 40 Hz. The stimulation intensity was ramped up over the first 60", kept constant through the entire session and ramped down over the last 60".

32-channel EEG data was recorded before and after each stimulation session using the Starstim device, allowing to monitor trajectory of change in gamma spectral power after each exposure to gamma-inducing tACS. Moreover, higher temporal and spatial resolution resting-state EEG was collected the week before and after the entire tACS treatment course (5' eyes open, 5' eyes closed) via a 64-channel actiCHamp EEG amplifier system (Brain Products GmbH), looking at changes in spectral power in three gamma sub-bands indexing low gamma (35–45 Hz), mid gamma (45–60 Hz), and gamma activity around the stimulation frequency (Stim γ=38–42 Hz), as well as slower oscillatory activity in the delta (1–4 Hz), theta (4–8 Hz), alpha (9–13 Hz), and beta bands (14–30 Hz).

Neuroimaging data acquisition

All enrolled subjects underwent separate PET and MRI visits. Participants underwent three PET imaging acquisitions both before and after the tACS treatment (Aβ, p-Tau, and microglia PET). The [^{11}C]-PiB, [^{18}F]-FTP, and [^{11}C]-PBR28 tracers were synthesized and administered onsite at the Gordon Center for Medical Imaging at Massachusetts General Hospital (MGH) in Boston, MA, USA. A 3-dimensional structural T1-weighted BRAVO sequence was acquired for anatomical reference using a 3T General Electrics (GE) MRI (repetition time = 8240 ms; echo time = 3.24 ms; inversion time = 450 ms; flip angle = 12°; voxel size = $0.94 \times 0.94 \times 1\ mm^3$ and matrix size = 256×256). MRI images were processed via FreeSurfer (FSv6.0) (http://surfer.nmr.mgh.harvard.edu) and manually

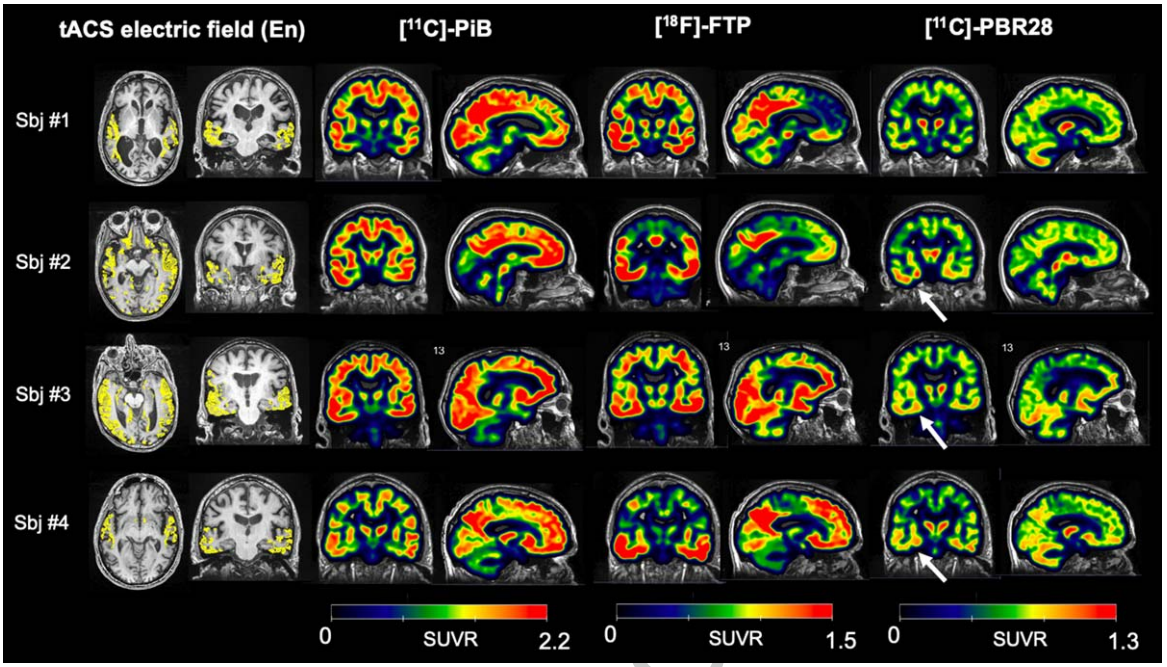

Fig. 2. tACS targets and SUVr parametric images for all participants. Axial and coronal views of the normal electric field induced by tACS in each participant are reported (yellow, En > 0.25 V/m on the structural MRI for anatomical reference), showing the tACS field affecting primarily the bilateral temporal lobes (left). Individual sagittal and coronal views of SUVr maps of [^{11}C]-PiB, [^{18}F]-FTP and [^{11}C]-PBR28 data collected at baseline for each patient are shown, displaying high levels of amyloid-β in all the participants, as well as significant p-Tau accumulation and signs of neuroinflammation (white arrows) in the bilateral temporal lobes, thalamus and parietal regions. Note: images are shown in radiological convention.

edited to improve cortical surfaces and define standard regions of interest (ROI) for PET analysis [32]. PET data were acquired on a Discovery MI (GE Healthcare) PET/CT scanner in static mode at 75–105 min post bolus injection of 10 mCi (370 MBq) for [^{18}F]-FTP [33], 50–70 min post bolus injection of 15 mCi (555 MBq) in the case of [^{11}C]-PiB [34], and 60–90 min post bolus injection of 15 mCi (555 MBq) for [^{11}C]-PBR28 [35].

A low dose X-ray CT scan was performed right before each PET segment for attenuation correction and was obtained with the GE MI Discovery PET/CT scanner. All PET/CT scans were completed within a 2-week period both preceding and following the tACS treatment.

Image processing

All PET processing was performed with an in-house developed Matlab software based on code and function from SPM8 (https://www.fil.ion.ucl.ac.uk/spm/software/spm8/) and FSL (https://fsl.fmrib.ox.ac.uk/fsl). PET images were motion corrected by realigning each frame to the first frame, co-registered to the corresponding baseline T1 image and FreeSurfer-derived ROIs were sampled.

PiB, FTP, and PBR28 retentions were expressed by standardized uptake values (SUV) normalized with a specific reference regions for each tracer (SUVr) providing more stable estimates for longitudinal studies [36]. Reference region-based analyses of [^{11}C]-PiB uptake were performed using the cerebellum cortex as a reference tissue [34], whereas for [^{18}F]-FTP the white matter was used instead [37, 33] and for [^{11}C]-PBR28 the uptake of the occipital cortex was employed. SUVr maps generated for these three tracers are shown in Fig. 2. Subjects were defined as Aβ positive if the global Aβ burden in a large neocortical aggregate (FS-derived "FLR" regions, composed by frontal, lateral parietal and temporal, and retrospenial regions) using PiB SUVr was equal to or greater than 1.25 [25, 38].

PET statistical analysis

The results are expressed as delta SUVr: percent change in SUVr from baseline to post-tACS follow-up. Test-retest reliability of PET measurement has

been demonstrated to be high, with a variability < 2% in the temporal lobes (Standard deviation, SD, at 4-week test-retest measurement = 1.97%) for [^{18}F]-FTP SUVr [39], and 3 to 5% for [^{11}C]-PiB SUVr [40]. As for [^{11}C]-PBR28, the cut-off of 2.47% determined by Nair et al. [41] when using the whole brain as reference region was used, as no test-retest study has been performed using the occipital cortex. Longitudinal comparison of individual SUVr data were interpreted as significant when showing a change (increase/decrease) higher than the aforementioned normative estimates of test-retest error.

RESULTS

Participants completed the study and tolerated the intervention without reporting any adverse events and attended 95% of the study visits (75/80 daily tACS visits, 5 sessions missed in total distributed across 3 patients), showing excellent treatment compliance even though the study required a high number of study visits (26 visits considering intervention and pre and post assessment visits) to be completed at the hospital (BIDMC, MGH). No seizures/signs of epileptiform activity were detected at the clinical assessment nor during the EEG recording post intervention.

EEG changes

When looking at pre-post tACS changes in EEG oscillatory activity, a trend for an increase in spectral power of gamma oscillations was found (Fig. 3A), with a stronger effect for oscillatory activity around the stimulation frequency (i.e., stim γ=38–42 Hz; Mann-Whitney $U = 3$, critical $U = 2$, $p = 0.186$). Analysis of daily EEG recordings indexing changes of gamma spectral power after each tACS session showed a pattern of increase in spectral power throughout each week of stimulation, with a partial reset of oscillatory activity during the weekends when stimulation was not performed (Fig. 3B). Such pattern was visible for stimulation electrodes (P7, P8, T7, T8) but not for control electrodes recording activity from frontal (AFz, F1, F2) and centro-parietal (C3, C4, Pz) regions of the brain.

P-Tau imaging

[^{18}F]-FTP PET revealed supra-threshold decreases of intracerebral p-Tau burden in temporal lobe regions targeted by tACS following the tACS treatment in 3/4 patients (Sbj #1 = 2.0%; Sbj #2 = –5.4%; Sbj #3 = –2.42%; Sbj #4 = –3.58%) (Fig. 3C, D). When looking closer at the sub-regions of the temporal lobe targeted by tACS and relevant for AD (i.e., mesial structures such as entorhinal cortex and parahippocampus) a group-level [^{18}F]-FTP PET binding decrease after the tACS treatment was observed (Supplementary Figure 1).

Microglia imaging

One subject displayed a significant decrease of microglia activation (Sbj #2 = –6.19%), paralleled by a significant decrease of p-Tau burden after the intervention (Sbj #2 = –5.4%). In the other 3 participants, changes were not significant (Sbj #1 = 2.30%; Sbj #3 = –0.38; Sbj #4 = 1.57) (Fig. 3C, D). However, when analyzing the group average changes on the stimulated temporal regions, a trend toward a decrease was found for the same mesial structures observed when analyzing p-Tau changes (Supplementary Figure 1).

Aβ imaging

[^{11}C]-PiB binding did not show any significant longitudinal changes considering that relative measurement error of the test-retest of Aβ-PET can reach 3–5% (Sbj #1 = –2.21%; Sbj #2 = –1.27%; Sbj #3 = –1.74%; Sbj #4 = 0.76%) (Fig. 3C).

Cognitive assessment

No significant changes in overall cognition were found after tACS using a Mann-Whitney non-parametric U test (ADAS-Cog baseline mean = 22.75, SD = 8.2, post = 24.6, SD = 11.4, Mann-Whitney $U = 12$, critical $U = 2$, p.=0.745; ADL baseline mean = 70, SD = 2.6, post = 70, SD = 3.5, Mann-Whitney $U = 12$, critical $U = 2$, $p. = 0.842$; MMSE baseline mean = 20.7, SD = 3.6, post = 20.5, SD = 3.4, Mann-Whitney $U = 12$, critical $U = 2$, $p. = 0.813$; MoCA: baseline mean = 13.25, SD = 4.1, post = 13.5, SD = 5.8, Mann-Whitney $U = 9$, critical $U = 2$, $p. = 0.725$), establishing safety of the tACS intervention.

DISCUSSION

Preliminary data from our case series suggest that 20 hours of daily gamma tACS distributed across 1 month is safe and tolerable in AD patients. A trend toward increase in gamma spectral power was

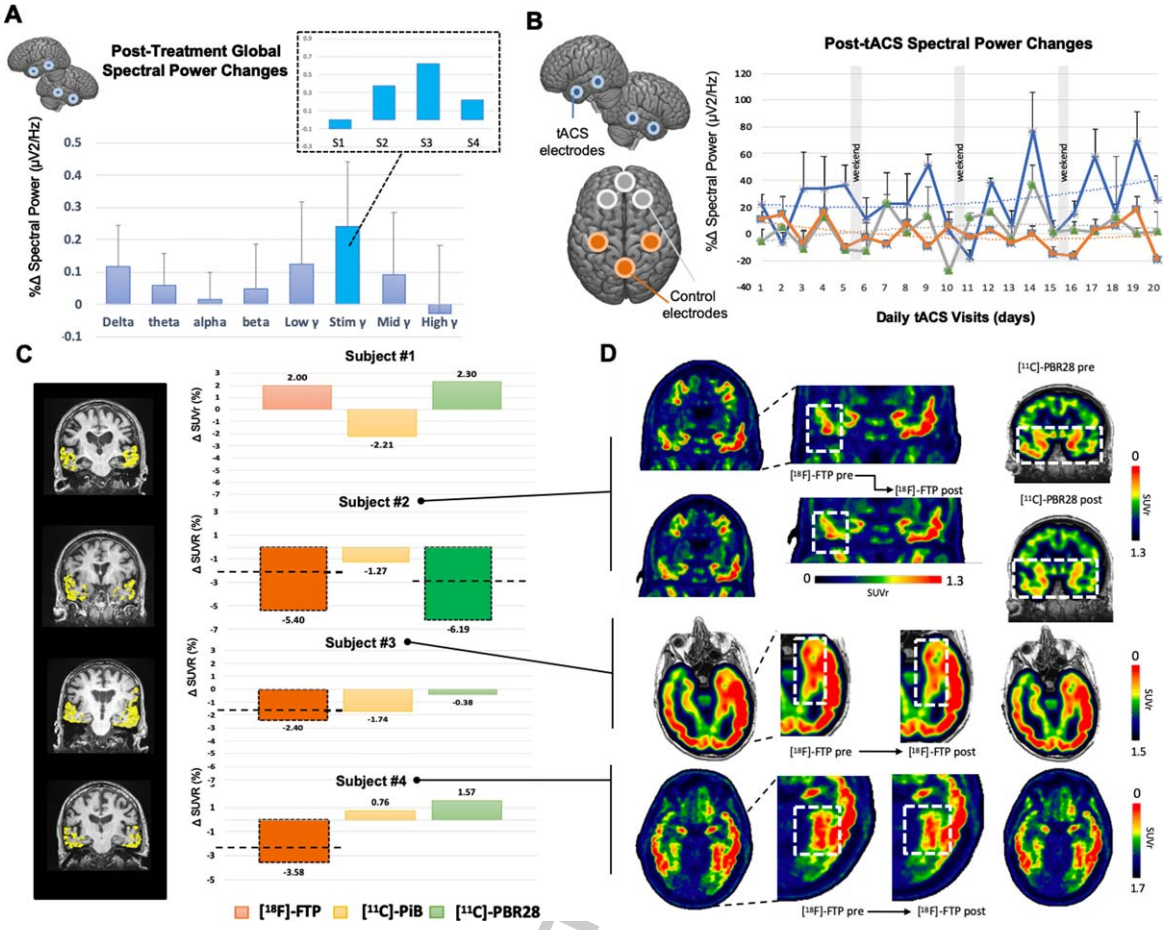

Fig. 3. Results. A) Participants reported a trend for an increase in spectral power of gamma oscillations, with a stronger effect for activity around the stimulation frequency (i.e., stim γ at 38–42 Hz). B) Daily EEG recordings before and after each tACS session showed an incremental effect of gamma spectral power over the stimulation electrodes placed on the temporal lobes (T8, P8, T7, P7), and no apparent changes in control electrodes indexing activity in frontal (Afz, F1, F2) and centro-parietal (C3, C4, Pz) regions. C) Delta SUVr between baseline and follow up are reported for the three PET tracers and specifically for SUVr values extracted from the individual tACS stimulation maps based on biophysical modeling (yellow, stimulation higher than 0.25 V/m). A significant (>1.98%) change in p-Tau deposition was observed for 3 patients (#2, #3, #4), as well as a decrease in microglia activation after tACS for patient #2. D) Individual data for participant #2, #3, and #4 showing example regions of putative change in p-Tau and microglia SUVr after tACS.

detected after the tACS intervention and 3/4 patients showed a decrease in p-Tau burden over the stimulated temporal lobe regions (Fig. 3). Pilot results are consistent with results obtained via optogenetic and sensory stimulation in the gamma band in preclinical models of AD [42]. However, we did not observe the originally predicted change in Aβ load based on the aforementioned results in a mouse model of AD. Considering the typical pattern of Aβ and p-Tau deposition in the human brain when patients are symptomatic—i.e., a diffuse Aβ pathology over the temporal, parietal, and prefrontal cortex in contrast with a p-Tau spread mostly affecting the temporal lobes (Fig. 2), we can speculate that gamma entrainment could be more effective on p-Tau rather than Aβ load in our study based on the specific tACS montage adopted [43]. In any case, we cannot completely rule out the possibility that the observed p-Tau burden decrease is due to intra-subject variability, even if thresholds for test-retest significance were defined according to most recent PET reliability literature. Further investigations on a bigger population are needed in order to determine the replicability of those current results since test-retest PET reliability thresholds have been determined based on studies with similar but not identical conditions.

Microglia show a neuroprotective role under physiological conditions [44], and there is mounting

evidence that neuroinflammation plays a critical role in the pathophysiology of AD [45]. In AD, microglia has been suggested to play a dual role, that is a positive effect on protein clearance when acutely activated, and a neurotoxic and pro-inflammatory one when chronically activated [46]. Even though the decrease observed in Sbj #3 could be in line with tACS reducing chronic hyperactivation in advanced AD patients, the lack of changes in the rest of the sample, as well as the non-significant changes in Aβ, could also be explained by a non-optimal window of observation, i.e., acutely after the intervention. Timing of sampling post-intervention is a key parameter to evaluate the impact of gamma-induction protocols and should be carefully considered in future studies. Regardless, the microglia-amyloid-tau crosstalk is still under investigation and clear pathophysiological cascades have not been identified yet. Interestingly, p-Tau and Aβ seem to colocalize in only the 0.02% of same synapses in the human brain and, even more intriguingly, microglia have been observed especially in proximity of p-Tau tangles [43]. These observations seem to suggest that microglia could have a more direct and effective action (i.e., clearance) on p-Tau aggregates rather than Aβ plaques because of this preferential colocalization. Furthermore, the PBR28 tracer has some limitations. TSPO is expressed throughout the brain, making the identification of a suitable reference region in PET analysis problematic. Also, the tracer seems to bind the pro-inflammatory phenotype of microglia (so called M1) but to some extent also the anti-inflammatory phenotype of microglia (called M2) [47]. The lack of a specific phenotype binding could have limited the detection of microglia activation changes in our sample. Overall, data suggest microglia PET imaging able to capture neuroinflammation in the temporal lobe in AD patients and promote its use for longitudinal evaluations of gamma-inducing protocols in AD.

The present study was conducted as a proof-of-principle of safety and feasibility in translating gamma-induction protocols used in animal models of AD to actual AD patients, including outcome measures related to protein clearance and neuroinflammation. The small sample was mostly due to the burden of multiple ($n = 6$) PET scans repeated over time and the long tACS treatment (average tACS exposure in literature is approximately 1 h per study, versus 20 h in the present protocol), and the study was not designed to show significant cognitive changes over a short 4-week window while at the same time providing valuable insight on the safety of sustained tACS delivery in AD patients. Given the demonstrated safety and feasibility, the dataset could be leveraged to design larger trials with even longer interventions (potentially in home-based settings), focusing on p-Tau pathology and neuroinflammation, and additional time points for PET imaging and/or blood markers. Importantly, the present pilot results support the safety and feasibility of applying a high dose of tACS (20 hours) for relatively long periods of time to broadly restore brain oscillations in AD. Interestingly, Slow Wave Activity (SWA, present in NREM sleep) as well as slow cortical oscillations (<1 Hz) are also impaired in AD, with preliminary evidences on AD mouse models showing how optogenetic restoration of SWA is able to inhibit Aβ accumulation and prevent calcium overload [48, 49]. Similar interventions via tACS could be implemented.

Conclusions

The study demonstrates preliminary evidence of safety, feasibility and potential impact of 40 Hz tACS on protein clearance in mild-to-moderate AD, promoting an interesting avenue of research in the quest for the identification of novel therapeutics for AD.

ACKNOWLEDGMENTS

The authors would like to thank patients and caregivers for their support and the Defense Advanced Research Projects Agency (DARPA) for their support to the study via HR001117S0030. Emiliano Santarnecchi is supported by the Beth Israel Deaconess Medical Center (BIDMC) via the Chief Academic Officer (CAO) Award 2017, the DARPA via HR001117S0030, the NIH (P01 AG031720-06A1, R01 MH117063-01, R01 AG060981-01), the Alzheimer's Drug Discovery Foundation (ADDF) and the Association for Frontotemporal Dementia (AFTD) via GA 201902-2017902.

The content is solely the responsibility of the authors and does not necessarily represent the official views of Harvard University, Harvard Medical School and their affiliated academic healthcare centers, or the National Institutes of Health.

APL and ES share a patent on the application of neuromodulation in Alzheimer's disease.

Authors' disclosures available online (https://www.j-alz.com/manuscript-disclosures/21-5072r1).

SUPPLEMENTARY MATERIAL

The supplementary material is available in the electronic version of this article: https://dx.doi.org/10.3233/JAD-215072.

REFERENCES

[1] Fratiglioni L, Launer LJ, Andersen K, Breteler MM, Copeland JR, Dartigues JF, Lobo A, Martinez-Lage J, Soininen H, Hofman A (2000) Incidence of dementia and major subtypes in Europe: A collaborative study of population-based cohorts. Neurologic Diseases in the Elderly Research Group. *Neurology* **54**, S10-15.

[2] Forester BP, Patrick RE, Harper DG (2020) Setbacks and opportunities in disease-modifying therapies in Alzheimer disease. *JAMA Psychiatry* **77**, 7-8.

[3] Bejanin A, Schonhaut DR, La Joie R, Kramer JH, Baker SL, Sosa N, Ayakta N, Cantwell A, Janabi M, Lauriola M, O'Neil JP, Gorno-Tempini ML, Miller ZA, Rosen HJ, Miller BL, Jagust WJ, Rabinovici GD (2017) Tau pathology and neurodegeneration contribute to cognitive impairment in Alzheimer's disease. *Brain* **140**, 3286-3300.

[4] Bartels T, De Schepper S, Hong S (2020) Microglia modulate neurodegeneration in Alzheimer's and Parkinson's diseases. *Science* **370**, 66-69.

[5] Jack CR, Wiste HJ, Lesnick TG, Weigand SD, Knopman DS, Vemuri P, Pankratz VS, Senjem ML, Gunter JL, Mielke MM, Lowe VJ, Boeve BF, Petersen RC (2013) Brain β-amyloid load approaches a plateau. *Neurology* **80**, 890-896.

[6] Pontecorvo MJ, Devous MD, Navitsky M, Lu M, Salloway S, Schaerf FW, Jennings D, Arora AK, McGeehan A, Lim NC, Xiong H, Joshi AD, Siderowf A, Mintun MA, 18F-AV-1451-A05 investigators (2017) Relationships between flortaucipir PET tau binding and amyloid burden, clinical diagnosis, age and cognition. *Brain* **140**, 748-763.

[7] Sanchez JS, Becker JA, Jacobs HIL, Hanseeuw BJ, Jiang S, Schultz AP, Properzi MJ, Katz SR, Beiser A, Satizabal CL, O'Donnell A, DeCarli C, Killiany R, El Fakhri G, Normandin MD, Gómez-Isla T, Quiroz YT, Rentz DM, Sperling RA, Seshadri S, Augustinack J, Price JC, Johnson KA (2021) The cortical origin and initial spread of medial temporal tauopathy in Alzheimer's disease assessed with positron emission tomography. *Sci Transl Med* **13**, eabc0655.

[8] Palop JJ, Mucke L (2010) Amyloid-beta-induced neuronal dysfunction in Alzheimer's disease: From synapses toward neural networks. *Nat Neurosci* **13**, 812-818.

[9] Babiloni C, Lizio R, Marzano N, Capotosto P, Soricelli A, Triggiani AI, Cordone S, Gesualdo L, Del Percio C (2016) Brain neural synchronization and functional coupling in Alzheimer's disease as revealed by resting state EEG rhythms. *Int J Psychophysiol* **103**, 88-102.

[10] Palop JJ, Mucke L (2016) Network abnormalities and interneuron dysfunction in Alzheimer disease. *Nat Rev Neurosci* **17**, 777-792.

[11] Iaccarino HF, Singer AC, Martorell AJ, Rudenko A, Gao F, Gillingham TZ, Mathys H, Seo J, Kritskiy O, Abdurrob F, Adaikkan C, Canter RG, Rueda R, Brown EN, Boyden ES, Tsai L-H (2016) Gamma frequency entrainment attenuates amyloid load and modifies microglia. *Nature* **540**, 230-235.

[12] Adaikkan C, Middleton SJ, Marco A, Pao P-C, Mathys H, Kim DN-W, Gao F, Young JZ, Suk H-J, Boyden ES, McHugh TJ, Tsai L-H (2019) Gamma entrainment binds higher-order brain regions and offers neuroprotection. *Neuron* **102**, 929-943.e8.

[13] Thomson H (2018) How flashing lights and pink noise might banish Alzheimer's, improve memory and more. *Nature* **555**, 20-22.

[14] Reed T, Cohen Kadosh R (2018) Transcranial electrical stimulation (tES) mechanisms and its effects on cortical excitability and connectivity. *J Inherit Metab Dis* **41**, 1123-1130.

[15] Santarnecchi E, Sprugnoli G, Bricolo E, Costantini G, Liew S-L, Musaeus CS, Salvi C, Pascual-Leone A, Rossi A, Rossi S (2019) Gamma tACS over the temporal lobe increases the occurrence of Eureka! moments. *Sci Rep* **9**, 5778.

[16] Santarnecchi, Polizzotto NR, Godone M, Giovannelli F, Feurra M, Matzen L, Rossi A, Rossi S (2013) Frequency-dependent enhancement of fluid intelligence induced by transcranial oscillatory potentials. *Curr Biol* **23**, 1449-1453.

[17] Jack CR, Wiste HJ, Botha H, Weigand SD, Therneau TM, Knopman DS, Graff-Radford J, Jones DT, Ferman TJ, Boeve BF, Kantarci K, Lowe VJ, Vemuri P, Mielke MM, Fields JA, Machulda MM, Schwarz CG, Senjem ML, Gunter JL, Petersen RC (2019) The bivariate distribution of amyloid-β and tau: Relationship with established neurocognitive clinical syndromes. *Brain* **142**, 3230-3242.

[18] Villemagne VL, Burnham S, Bourgeat P, Brown B, Ellis KA, Salvado O, Szoeke C, Macaulay SL, Martins R, Maruff P, Ames D, Rowe CC, Masters CL, Australian Imaging Biomarkers and Lifestyle (AIBL) Research Group (2013) Amyloid β deposition, neurodegeneration, and cognitive decline in sporadic Alzheimer's disease: A prospective cohort study. *Lancet Neurol* **12**, 357-367.

[19] Frohlich F, McCormick DA (2010) Endogenous electric fields may guide neocortical network activity. *Neuron* **67**, 129-143.

[20] Tatti E, Rossi S, Innocenti I, Rossi A, Santarnecchi E (2016) Non-invasive brain stimulation of the aging brain: State of the art and future perspectives. *Ageing Res Rev* **29**, 66-89.

[21] Nedergaard M, Goldman SA (2020) Glymphatic failure as a final common pathway to dementia. *Science* **370**, 50-56.

[22] Santarnecchi, Muller T, Rossi S, Sarkar A, Polizzotto NR, Rossi A, Cohen Kadosh R (2016) Individual differences and specificity of prefrontal gamma frequency-tACS on fluid intelligence capabilities. *Cortex* **75**, 33-43.

[23] Santarnecchi E, Biasella A, Tatti E, Rossi A, Prattichizzo D, Rossi S (2017) High-gamma oscillations in the motor cortex during visuo-motor coordination: A tACS interferential study. *Brain Res Bull* **131**, 47-54.

[24] Klunk WE, Engler H, Nordberg A, Wang Y, Blomqvist G, Holt DP, Bergström M, Savitcheva I, Huang G, Estrada S, Ausén B, Debnath ML, Barletta J, Price JC, Sandell J, Lopresti BJ, Wall A, Koivisto P, Antoni G, Mathis CA, Långström B (2004) Imaging brain amyloid in Alzheimer's disease with Pittsburgh Compound-B. *Ann Neurol* **55**, 306-319.

[25] Johnson KA, Schultz A, Betensky RA, Becker JA, Sepulcre J, Rentz D, Mormino E, Chhatwal J, Amariglio R, Papp K, Marshall G, Albers M, Mauro S, Pepin L, Alverio J, Judge K, Philiossaint M, Shoup T, Yokell D, Dickerson B, Gomez-Isla T, Hyman B, Vasdev N, Sperling R (2016) Tau positron emission tomographic imaging in aging and early Alzheimer disease. *Ann Neurol* **79**, 110-119.

[26] Kreisl WC, Lyoo CH, McGwier M, Snow J, Jenko KJ, Kimura N, Corona W, Morse CL, Zoghbi SS, Pike VW, McMahon FJ, Turner RS, Innis RB, Biomarkers Consortium

PET Radioligand Project Team (2013) *In vivo* radioligand binding to translocator protein correlates with severity of Alzheimer's disease. *Brain* **136**, 2228-2238.

[27] Rosen WG, Mohs RC, Davis KL (1984) A new rating scale for Alzheimer's disease. *Am J Psychiatry* **141**, 1356-1364.

[28] Folstein MF, Folstein SE, McHugh PR (1975) "Mini-mental state". A practical method for grading the cognitive state of patients for the clinician. *J Psychiatr Res* **12**, 189-198.

[29] Nasreddine ZS, Phillips NA, Bédirian V, Charbonneau S, Whitehead V, Collin I, Cummings JL, Chertkow H (2005) The Montreal Cognitive Assessment, MoCA: A brief screening tool for mild cognitive impairment. *J Am Geriatr Soc* **53**, 695-699.

[30] Galasko D, Bennett D, Sano M, Ernesto C, Thomas R, Grundman M, Ferris S (1997) An inventory to assess activities of daily living for clinical trials in Alzheimer's disease. The Alzheimer's Disease Cooperative Study. *Alzheimer Dis Assoc Disord* **11**(Suppl 2), S33-39.

[31] Wessels AM, Lines C, Stern RA, Kost J, Voss T, Mozley LH, Furtek C, Mukai Y, Aisen PS, Cummings JL, Tariot PN, Vellas B, Dupre N, Randolph C, Michelson D, Andersen SW, Shering C, Sims JR, Egan MF (2020) Cognitive outcomes in trials of two BACE inhibitors in Alzheimer's disease. *Alzheimers Dement* **16**, 1483-1492.

[32] Desikan RS, Ségonne F, Fischl B, Quinn BT, Dickerson BC, Blacker D, Buckner RL, Dale AM, Maguire RP, Hyman BT, Albert MS, Killiany RJ (2006) An automated labeling system for subdividing the human cerebral cortex on MRI scans into gyral based regions of interest. *Neuroimage* **31**, 968-980.

[33] Baker SL, Maass A, Jagust WJ (2017) Considerations and code for partial volume correcting [18F]-AV-1451 tau PET data. *Data Brief* **15**, 648-657.

[34] McNamee RL, Yee S-H, Price JC, Klunk WE, Rosario B, Weissfeld L, Ziolko S, Berginc M, Lopresti B, Dekosky S, Mathis CA (2009) Consideration of optimal time window for Pittsburgh compound B PET summed uptake measurements. *J Nucl Med* **50**, 348-355.

[35] Lyoo CH, Ikawa M, Liow J-S, Zoghbi SS, Morse CL, Pike VW, Fujita M, Innis RB, Kreisl WC (2015) Cerebellum can serve as a pseudo-reference region in Alzheimer disease to detect neuroinflammation measured with PET radioligand binding to translocator protein. *J Nucl Med* **56**, 701-706.

[36] Lopresti BJ, Klunk WE, Mathis CA, Hoge JA, Ziolko SK, Lu X, Meltzer CC, Schimmel K, Tsopelas ND, DeKosky ST, Price JC (2005) Simplified quantification of Pittsburgh Compound B amyloid imaging PET studies: A comparative analysis. *J Nucl Med* **46**, 1959-1972.

[37] Hanseeuw BJ, Betensky RA, Jacobs HIL, Schultz AP, Sepulcre J, Becker JA, Cosio DMO, Farrell M, Quiroz YT, Mormino EC, Buckley RF, Papp KV, Amariglio RA, Dewachter I, Ivanoiu A, Huijbers W, Hedden T, Marshall GA, Chhatwal JP, Rentz DM, Sperling RA, Johnson K (2019) Association of amyloid and tau with cognition in preclinical Alzheimer disease: A longitudinal study. *JAMA Neurol* **76**, 915-924.

[38] Bullich S, Seibyl J, Catafau AM, Jovalekic A, Koglin N, Barthel H, Sabri O, De Santi S (2017) Optimized classification of 18F-Florbetaben PET scans as positive and negative using an SUVR quantitative approach and comparison to visual assessment. *Neuroimage Clin* **15**, 325-332.

[39] Devous MD, Joshi AD, Navitsky M, Southekal S, Pontecorvo MJ, Shen H, Lu M, Shankle WR, Seibyl JP, Marek K, Mintun MA (2018) Test-retest reproducibility for the tau PET imaging agent Flortaucipir F 18. *J Nucl Med* **59**, 937-943.

[40] Heeman F, Hendriks J, Lopes Alves I, Ossenkoppele R, Tolboom N, van Berckel BNM, Lammertsma AA, Yaqub M, AMYPAD Consortium (2020) [11C]PIB amyloid quantification: Effect of reference region selection. *EJNMMI Res* **10**, 123.

[41] Nair A, Veronese M, Xu X, Curtis C, Turkheimer F, Howard R, Reeves S (2016) Test-retest analysis of a non-invasive method of quantifying [(11)C]-PBR28 binding in Alzheimer's disease. *EJNMMI Res* **6**, 72.

[42] Martorell AJ, Paulson AL, Suk H-J, Abdurrob F, Drummond GT, Guan W, Young JZ, Kim DN-W, Kritskiy O, Barker SJ, Mangena V, Prince SM, Brown EN, Chung K, Boyden ES, Singer AC, Tsai L-H (2019) Multi-sensory gamma stimulation ameliorates Alzheimer's-associated pathology and improves cognition. *Cell* **177**, 256-271.e22.

[43] Busche MA, Hyman BT (2020) Synergy between amyloid-β and tau in Alzheimer's disease. *Nat Neurosci* **23**, 1183-1193.

[44] Nimmerjahn A, Kirchhoff F, Helmchen F (2005) Resting microglial cells are highly dynamic surveillants of brain parenchyma *in vivo*. *Science* **308**, 1314-1318.

[45] Leng F, Edison P (2021) Neuroinflammation and microglial activation in Alzheimer disease: Where do we go from here? *Nat Rev Neurol* **17**, 157-172.

[46] Liddelow SA, Guttenplan KA, Clarke LE, Bennett FC, Bohlen CJ, Schirmer L, Bennett ML, Münch AE, Chung W-S, Peterson TC, Wilton DK, Frouin A, Napier BA, Panicker N, Kumar M, Buckwalter MS, Rowitch DH, Dawson VL, Dawson TM, Stevens B, Barres BA (2017) Neurotoxic reactive astrocytes are induced by activated microglia. *Nature* **541**, 481-487.

[47] Liu B, Le KX, Park M-A, Wang S, Belanger AP, Dubey S, Frost JL, Holton P, Reiser V, Jones PA, Trigg W, Di Carli MF, Lemere CA (2015) *In vivo* detection of age- and disease-related increases in neuroinflammation by 18F-GE180 TSPO microPET imaging in wild-type and Alzheimer's transgenic mice. *J Neurosci* **35**, 15716-15730.

[48] Kastanenka KV, Hou SS, Shakerdge N, Logan R, Feng D, Wegmann S, Chopra V, Hawkes JM, Chen X, Bacskai BJ (2017) Optogenetic restoration of disrupted slow oscillations halts amyloid deposition and restores calcium homeostasis in an animal model of Alzheimer's disease. *PLoS One* **12**, e0170275.

[49] Lee YF, Gerashchenko D, Timofeev I, Bacskai BJ, Kastanenka KV (2020) Slow wave sleep is a promising intervention target for Alzheimer's disease. *Front Neurosci* **14**, 705.